Time-resolved measurements of ion energy distributions and optical emissions in pulsed radio-frequency discharges

Yicheng Wang,[a] Eric C. Benck, Martin Misakian, Manabu Edamura, and James K. Olthoff

National Institute of Standards and Technology, Gaithersburg, Maryland 20899

In pulse-modulated inductively coupled plasmas generated in CF_4:Ar mixtures, a transition between a capacitive coupling mode (E mode) and an inductive coupling mode (H mode) was observed. For a pulsed plasma in a 50%CF_4:50%Ar volume mixture with a peak rf power of 200 W at 13.56 MHz and a modulation frequency at 500 Hz with a duty cycle of 95%, the $E \rightarrow H$ mode transition occurs repetitively 0.75 ms after each rf pulse is applied. This long delay in the mode transition allows us to perform not only time-resolved measurements of optical emission and electrical characteristics but also time-resolved measurements of ion energy distributions at the grounded electrode. These measurements show that a relatively short rf off period can severely perturb the equilibrium plasma state and its recovery may take much longer than the rf off period. [S0021-8979(00)02805-X]

I. INTRODUCTION

It has recently been suggested that pulsed power modulation of high density plasmas could be used to gain additional control over plasma properties and thus improve the etch results. For example, Samukawa[1] has shown that pulsing the power to a CHF_3 electron cyclotron resonance plasma greatly enhanced selectivity of SiO_2 etching on Si. The selectivity increase was attributed to the relative increase of heavy radicals such as CF_2 and CF_3. Sugai *et al.*[2] suggested that the momentary removal of plasma sheaths in pulsed high-density inductively coupled plasmas (ICPs) helped suppress charge buildup on high-aspect-ratio micropatterns. The suppression of charge buildup was attributed in part to the enhanced negative ion yield resulting from electron cooling in the afterglow and the resultant change in sheath dynamics.[3] Pulse modulation of plasma sources also provides additional control variables to study plasma physics and chemistry, as evidenced by the recent surge of activities in this area.[4–6]

The objective of our work is to examine the fundamental characteristics of pulsed plasmas and to develop diagnostic methods for plasma process control suitable for pulse-modulated ICPs containing CF_4. CF_4 is a commonly used gas for the plasma etching of Si and SiO_2 surfaces, and for plasma chamber cleaning processes when mixed with oxygen. In this article, we report time-resolved measurements of ion energy distributions and relative ion densities at the grounded electrode of an ICP gaseous electronics conference (GEC) rf reference cell (RC) for pulse-modulated discharges in CF_4:Ar mixtures. It is shown for pulsed plasmas containing CF_4, that time-resolved mass analysis of ion flux is essential since the relative abundance of ionic species varies strongly with time. Time-resolved measurements of optical emission and electrical characteristics are also presented.

II. EXPERIMENTAL APPARATUS

Plasmas were generated in a GEC rf reference reactor[7] whose upper electrode was replaced with a five-turn planar rf-induction coil behind a quartz window to produce inductively-coupled discharges.[8] The reactor, along with the ion-energy analyzer and mass spectrometer, has been described in detail previously.[9] The feed gas enters the cell through a 70 mm side flange and is pumped out through a 152 mm port attached to a turbomolecular pump. The gas pressure is maintained by a variable conductance gate valve between the pump and the GEC cell. The flow was maintained by mass flow controllers at 7.45 μmol/s (10 sccm) for all of the experiments reported here.

For pulsed operation, the rf power to the inductive coil was supplied by a rf amplifier with its input connected to a wave form synthesizer operating at 13.56 MHz. A master gate pulse generator with variable pulse repetition rate and duty cycle was used to gate the rf output and synchronize all time-resolved measurements. Because the plasma and the corresponding impedance continually changes, it is impossible for the matching network to be continuously optimized with a pulsed plasma. In order to obtain reproducible matching conditions, the matching network was optimized for the case of continuous excitation. The rf power values presented in this article are the net power to the matching network driving the coil under continuous excitation. The actual rf power dissipated in a continuous plasma has been determined to be approximately 80% of the net power. The lower electrode was grounded to the vacuum chamber.

Electrical measurements for the plasma were made using homebuilt voltage and current probes attached to the leads of the rf induction coil. These homebuilt probes were calibrated against commercially available probes. The transient voltage and current signals were recorded with a digital oscilloscope. The digital oscilloscope was operated in the envelope mode so that only the maximum amplitudes of the rf current and

[a] Electronic mail: wang@eeel.nist.gov

voltage were recorded. This was necessary since there was no synchronization between the rf and discharge pulsing.

The time-resolved optical emission measurements were made utilizing a 1 m monochromator with a photomultiplier detector and computer controlled mirror collection optics which have been described previously.[10] The observation region in the plasma was 12 mm above the lower electrode. The photomultiplier signal was recorded and averaged over as many as 5000 pulses with a digital oscilloscope. In order to improve the oscilloscope averaging, the 5 ns long photoelectric pulses were stretched to a few tens of nanoseconds with a simple RC integrator.

The ion sampling arrangement is the same as that used to study ICPs generated in CF_4 under continuous excitation.[9,11] Ions are sampled through a 10 μm diameter orifice in a 2.5-μm-thick nickel foil that was spot welded into a small counter bore in the center of the stainless steel lower electrode. For ion energy distribution (IED) measurements, the ions that pass through the orifice are accelerated and focused into a 45° electrostatic energy selector. After being selected according to their energy, the ions enter a quadrupole rf mass filter where they are also selected according to their mass-to-charge ratio. The resolution of the electrostatic analyzer was fixed at a value of 1 eV, full width at half maximum, and the uncertainty in the energy scale is estimated to be ± 1.0 eV. Time-resolved IED measurements were achieved by gating the digital ion counting pulses from the electron multiplier. The gating pulse, which was 0.1 ms for this work, was synchronized to the master gate pulse generator through a variable digital delay generator.

Past experience with the ion-energy analyzer[12] indicates that the ion transmission is uniform over the ion energy ranges observed here. The mass spectrometer was tuned such that the ion transmission was nearly constant over the range of ion masses detected here (12–40 u), however, a transmission correction factor was applied to the highest mass ions (mass >40 u) to compensate for some decrease in ion transmission with increasing mass.[9]

III. RESULTS AND DISCUSSION

A. Electrical measurements

Typical induction coil voltage and current waveforms are shown in Fig. 1 for a pulsed plasma at 500 Hz with a duty cycle of 95% (the rf off time equal to 0.1 ms), 200 W, and 2.67 Pa of 50%CF_4:50%Ar. As the pulsed power is applied, the discharge ignites in the dim or E mode (0.1–0.85 ms) and then makes a transition into the bright or H mode (0.85–2.0 ms). For the pulsing conditions being studied, these plasmas remain in the E mode for a significantly longer time (750 μs) than previously reported in other types of pulsed plasmas (100 μs in Ar and 2 μs in Cl_2).[8,13] The E mode is characterized by higher voltage and currents than those found in the H mode. Even though the voltage and current are higher than the H mode, the corresponding power deposited into the plasma is much lower. This is due to increased reflected power and increased power loss in the coil ($I^2 R_{eff}$).
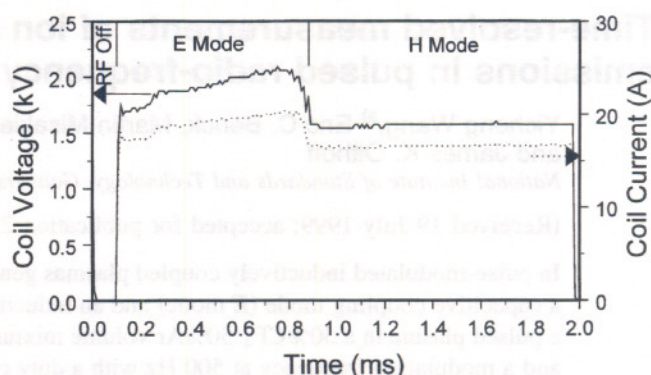

FIG. 1. Electrical parameters (rf voltage and current amplitudes at the rf induction coil leads) of the pulsed Ar:CF_4 discharge (500 Hz with a duty cycle of 95%, 200 W, 2.67 Pa, 7.4 μmol/s).

B. Optical measurements

Optical emission measurements of the pulsed plasma were made at several wavelengths corresponding to transitions from both Ar at $\lambda = 750.4$ nm ($4s'[1/2]°-4p'[1/2]$, $E_{threshold} = 13.48$ eV) and $\lambda = 419.8$ nm ($4s[3/2]°-5p[1/2]$, $E_{threshold} = 14.57$ eV) and F at $\lambda = 775.5$ nm ($3s^2 P_{3/2}-3p^2 D°_{5/2}$, $E_{threshold} = 14.58$ eV) excited states. Typical optical emission signals obtained under the same plasma conditions as in Fig. 1 are shown in Fig. 2. Optical emission in the H mode is approximately 80 times more intense than in the E mode. When the plasma makes the transition into the H mode, the Ar emission overshoots and then oscillate several times before reaching a constant value around 1.4 ms. The observed fluorine optical emission is approximately two orders of magnitude less intense than the observed Ar transition. Although an increased light output from F is evident during the E mode over that observed
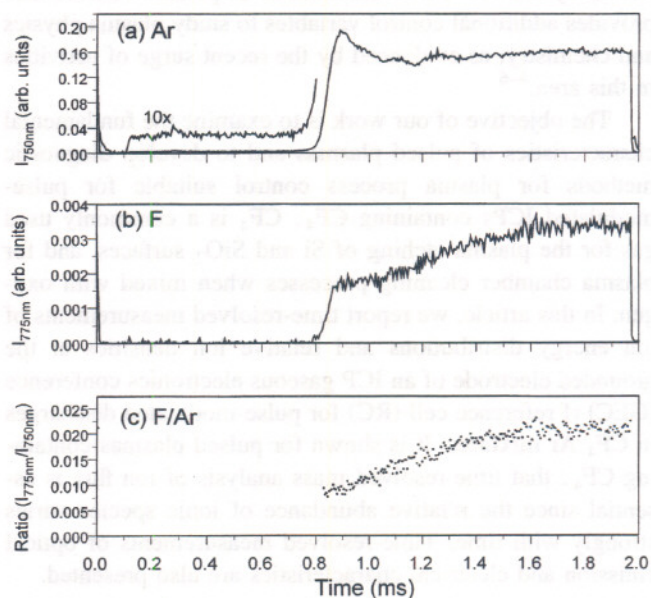

FIG. 2. Optical emission measurements of the pulsed Ar:CF_4 discharge (500 Hz with a duty cycle of 95%, 200 W, 2.67 Pa, 7.4 μmol/s). (a) Ar emissions at 750.4 nm, (b) F emissions at 775.4 nm, and (c) ratio of F(775.4 nm)/Ar(750.4 nm).
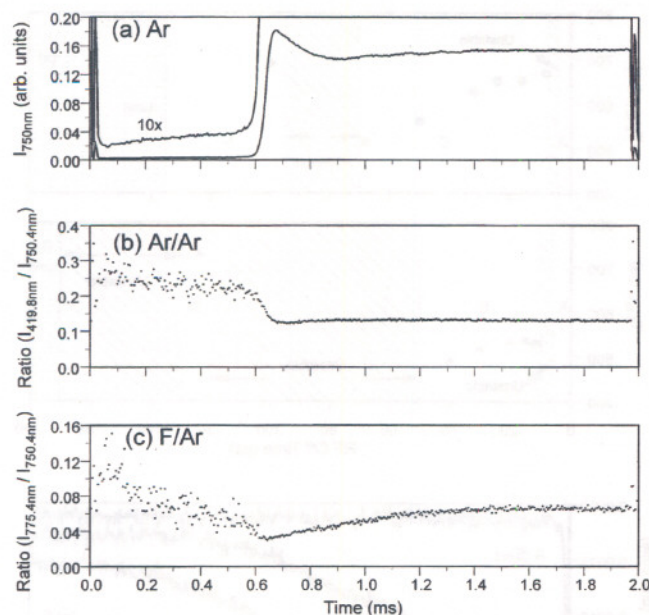
FIG. 3. Optical emission measurements of the pulsed Ar:CF$_4$ discharge (500 Hz with a duty cycle of 99.525%, 200 W, 2.67 Pa, 7.4 μmol/s). (a) Ar emissions at 750.4 nm, (b) ratio of Ar(419.8 nm)/Ar(750.4 nm), and (c) ratio of F(775.4 nm)/Ar(750.4 nm).

FIG. 4. Detail of the optical emission measurements of the pulsed Ar:CF$_4$ discharge (500 Hz with a duty cycle of 99.525%, 200 W, 2.67 Pa, 7.4 μmol/s). (a) Ar emissions at 419.8 nm, (b) F emissions at 775.4 nm, and (c) rf voltage amplitude at the coil.

during the preceding afterglow plasma (<0.1 ms), the light intensity is too small to be accurately averaged.

A ratio of the fluorine and argon emissions ($I_{775 nm}/I_{750 nm}$) during the H mode is shown in Fig. 2(c). The ratio during the E mode has not been included since the signal-to-noise ratio of the F emissions during the E mode is very poor. This ratio should approximately reflect the relative fluorine density by canceling out effects due to the varying electron density and temperature, assuming that contributions to the excited Ar* and F* production from other processes such as two step excitation and variations in the excitation rate coefficients with electron temperature are small. Argon metastable densities in the GEC–ICP RC are typically low enough so that direct electron excitation from the ground state dominates two step processes,[14,15] and fluorine metastable densities are also typically very low due to a forbidden transitions to the ground state.[16] Time resolved Langmuir probe measurements indicate that the electron temperature does not significantly vary during the H mode and thus differences in the dependence on the electron temperature of the Ar and F excitation rates should not be a factor. Therefore, the ratio suggests that there is a steady increase in the F density until approximately 1.6 ms, where a relatively constant density is obtained. This indicates that there is a significant time lag between the rapid increase in electron density which should occur during the start of the H mode and the consequential increase in F density.

Figure 3(a) shows the Ar optical emissions from a similar plasma with a shorter rf off time (0.01 ms) with all other plasma conditions the same as in Fig. 1. The optical emission wave form is qualitatively similar to that obtained with the longer rf interruption, with the exception of a small peak occurring when the rf power is turned back on (9.5 μs). The discharge appears to be attempting to restart into the H

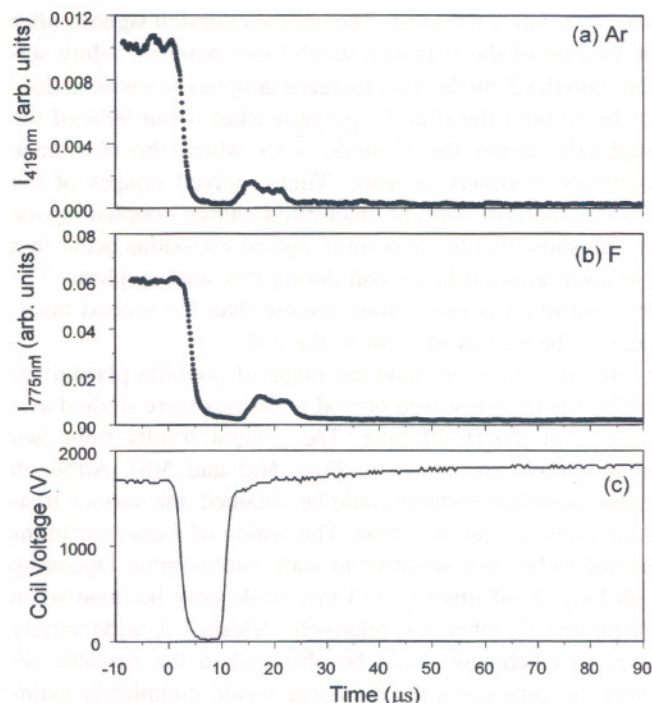mode, but is unable to sustain this mode and continues in the E mode. Figures 3(b) and 3(c) are ratios of the optical emissions from an argon ($\lambda = 419.8$ nm) and fluorine ($\lambda = 775.4$ nm) excited state with the 750.4 nm Ar transition. Because the threshold values for these two argon states are close, it is necessary to consider the full electron excitation cross section to determine how the argon ratio depends on electron temperature. Convoluting Maxwellian electron distribution functions with electron excitation cross sections,[17] it can be shown that the ratio $I_{419 nm}/I_{750 nm}$ is a monotonically increasing function of the electron temperature (T_e) in the region of interest (0.25–10 eV). The ratios of many other transitions with similar or even higher threshold energies than the $5p[1/2]$ state (14.57 eV) actually decrease with increasing T_e. Therefore, assuming that direct excitation from ground state is the dominant excitation process, the ratio in Fig. 3(b) should monitor changes in the temperature of high energy electrons within the plasma. The higher ratio in the E vs H mode indicates a higher effective electron temperature in the E mode. The fluorine emissions from this plasma were more intense than in Fig. 2 so that a reasonable signal-to-noise ratio could be obtained during both the E and H modes. The $I_{775 nm}/I_{750 nm}$ ratio continues to decrease during the E mode, suggesting that the density of F radicals continues to decrease in the E mode. This decrease can be attributed to the much lower equilibrium plasma density in the E mode than in the H mode. The ratio increases during the H mode, similar to Fig. 2(c).

The turn-on behavior of this plasma is shown in more detail in Fig. 4. Figures 4(a) and 4(b) are optical emission signals from Ar* and F*, respectively. Both signals show the

same qualitative behavior. The optical emission signals, after the turn on of the rf power, exhibit two maxima before settling into the E mode. This increase in optical emissions does not begin until the rf coil voltage reaches about 90% of the amplitude during the H mode, after which the rf voltage continues to slowly increase. Time-resolved images of the plasma obtained using an intensified charge coupled device camera show that the maximum optical emissions occur in a thin layer adjacent to the coil during this start up phase. The first maximum is much more intense than the second maximum in the region adjacent to the coil.

In order to understand the range of possible plasma behavior, the time-resolved optical emissions were studied as a function of the rf off time. The general results from two separate days are shown in Figs. 5(a) and 5(b). Although similar emission patterns could be obtained, the various transition times are not the same. The timing of these transitions seemed to be very sensitive to wall conditioning. Operating with long rf off times (~ 0.3 ms) could only be done when the plasma chamber was relatively "clean." A wide variety of plasma behavior could be observed in the unstable regions. In some cases the discharge would completely extinguish after several seconds of operation. A more common instability involved large fluctuations in the transition time from the E to H mode. Occasionally, the plasma even had a type of period doubling where the E to H mode transition would occur every other pulse cycle.

There were three distinct regions of stable plasma operation for which the characteristic optical emission wave forms are shown in Fig. 5(c). In region A, there is essentially no E mode, with the optical emissions rapidly approaching the H mode intensity. In region B, there is a relatively long E mode. The time from the turn on of the rf power until the E to H mode transition decreases with increasing rf off time (decreasing duty cycle). The wave forms for the shorter rf off times in this region exhibit a local maximum immediately after the rf power is turned on, similar to Fig. 4. The peak value of this local maximum decreases with increasing rf off time and eventually disappears. The final amplitude of the H mode from the fluorine emissions (775.5 nm) decreases with increasing rf off time, while there was no such trend in the argon emissions (750.4 nm), indicating that the F density decreases with increasing rf off time. In region C, the time spent in the E mode has significantly increased. The decreased slope of the optical emissions during the E to H mode transition may actually be an indication that the transition time is becoming unstable and smeared due to the signal averaging. Also the optical emissions are significantly lower than in region B.

The exact reason why there is such a long delay in region B and C before the E to H mode transition is not clear. It has been proposed that the E to H mode transition as a function of rf power in continuous ICP discharges is due to nonlinear power absorption as a function of electron density.[18–20] In the pulsed plasmas investigated here, the electron density is influenced by other time-dependent factors such as the densities of argon metastables and radicals of CF_4. It is important to note that although CF_4 is a weakly electron attaching gas, its radicals and other discharge by-
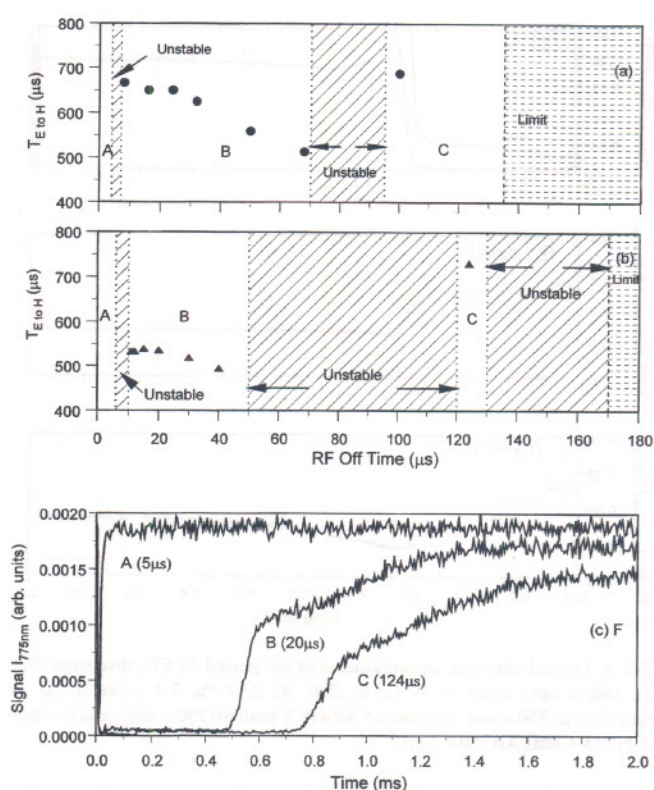

FIG. 5. Time delay from the turn on of rf power to the start of the H mode vs the rf off time for identical Ar:CF_4 discharges (200 W, 2.67 Pa, 7.4 μmol/s) from two separate days: (a) February 8, 1999, (b) April 13, 1999. (c) Characteristic optical emission wave forms F(775.5 nm) for the different rf off ranges measured on April 13, 1999.

products could be strongly electron attaching. As the free electrons quickly cool off during the afterglow, the electron attachment rate may significantly increase, resulting in a space charge dominated by negative and positive ions. This kind of space charge can contribute to the delay in the E to H mode transition because it increases the electron loss rate. Changes in wall recombination rates may also explain the sensitivity of the pulsed plasma behavior to the wall and electrode surface conditions.

C. Ion energy distributions

Ion energy measurements typically have much lower time resolution than optical and electrical measurements. Nevertheless, the "delayed" $E \rightarrow H$ mode transition allows us to perform time-resolved IED measurements. Figure 6(a) shows the integrated ion intensities of Ar^+, CF_3^+, CF_2^+, and CF^+ as a function of the gate delay time, t. All results presented in this section were obtained under the same plasma conditions as in Fig. 1, i.e., for a pulsed plasma at 500 Hz with a duty cycle of 95% (the rf off time equal to 0.1 ms), 200 W, and 2.67 Pa of 50%CF_4:50%Ar. The sum of the intensities of other ion species including C^+, F^+, and CO^+ which are not shown in the figure represents less than 5% of the total ion intensity. The transit time through the mass-analyzer system for the ions shown in Fig. 6 is slightly more than 0.1 ms. Thus, the data shown in Fig. 6(a) for $t=0$ represent ion intensities in a plasma with rf power still fully
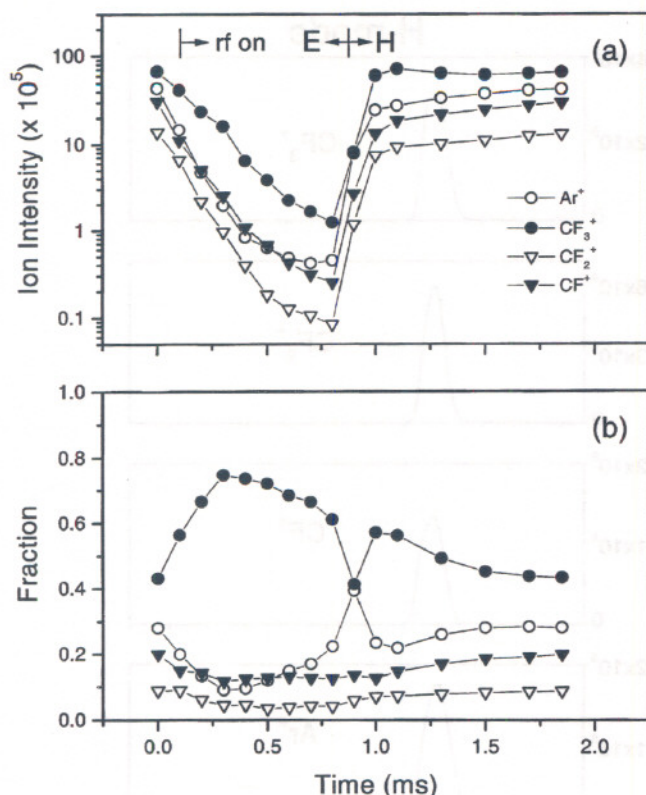
2118   J. Appl. Phys., Vol. 87, No. 5, 1 March 2000

Wang *et al.*

FIG. 6. (a) Integrated intensities of Ar^+, CF_3^+, CF_2^+, and CF^+ ions sampled through a 10 μm diameter orifice at the grounded electrode in a 0.1 ms time window as a function of the gate delay time with the same plasma conditions as Fig. 1. (b) Fraction of these ions (the same symbols) as a function of time.

on and the plasma in the H mode. As t increases, the intensities of all ions decrease rapidly until the $E-H$ mode transition occurs. It is interesting to note that the intensity decrease continues in the region where the rf power is already back on and the plasma is well in the dim mode as evidenced by the optical emission measurements. This decrease, similar to the observed decrease of the F density, can be attributed to the much lower equilibrium plasma density in the E mode than that in the H mode. The transition to the H mode occurs rapidly and is complete at $t=1.0$ ms. Thereafter, the intensities of Ar^+, CF_2^+, and CF^+ increase gradually. The intensity of CF_3^+, on the other hand, appears to overshoot slightly and decreases after $t=1.1$ ms before reaching a plateau. Figure 6(b) shows the percentage of the four dominant ions as a function of the delay time. As can be seen, while CF_3^+ is the dominant ion overall, its fraction decreases from as high as 74% in the E mode to about 44% in the H mode. The rapid increase of CF_3^+ percentage from $t=0$ to $t=0.3$ ms is accompanied by the rapid decrease of Ar^+, partly due to large charge transfer cross section for collisions of Ar^+ with CF_4 yielding CF_3^+ ($\sim$ 100 $Å^2$ at 0.1 eV collision energy).[21] The fraction of Ar^+ increases rapidly as the transition approaches, which could be due to the increase of Ar metastables which have a much lower ionization potential than the ground state.

Typical IEDs for CF_3^+, CF_2^+, CF^+, and Ar^+ acquired in the E mode at $t=0.7$ ms are shown in Fig. 7 together with

IEDs of these ions obtained in the H mode at $t=1.5$ ms. The IEDs in the H mode for these ions are similar to each other and show a featureless single peak at 16 eV and with a half peak width about 3–4 eV. These IEDs are similar in shape to the IEDs reported earlier for CF_4:Ar plasmas under continuous rf excitation.[11] The IEDs in the E mode, however, differ dramatically from the IEDs in the H mode. First, the relative intensities are lower by almost two orders of magnitude. Second, the average ion energies are much higher, indicating that the plasma potential is significantly higher in the E mode. The increase of the plasma potential can be attributed in part to an increased rf voltage drop across the ground sheath.[22] The increase can also be partly due to an increase of the electron temperature. Such an increase of the electron temperature in the E mode was previously observed in pulsed, inductively coupled Ar and Cl_2 plasmas.[6] The IEDs of CF_3^+, CF_2^+, and CF^+ are characterized by a double peak centered around 40 eV. IEDs of this shape are often observed in capacitively-coupled plasmas and are caused by rf modulation of the plasma potential across the sheath. In the present case, the double peaked IEDs suggest that the amplitude of rf component of the plasma potential across the ground sheath increases significantly in the E mode. The much lower plasma density together with the higher plasma potential in the E mode leads to a thicker ground sheath according to the Child–Langmuir law,[23] resulting in a smaller ground sheath capacitance. The smaller ground sheath capacitance in turn leads to a larger rf potential across the sheath because the capacitance between the rf coil and the plasma is largely fixed by the quartz window between them. The separation between the two peaks increases from CF_3^+ to CF^+, which is consistent with the notion that the lighter ions are influenced more by the rf modulation across the sheath. The IED of Ar^+ is different from those of CF_4 fragment ions. In addition to the double peaked structure centered at 40 eV, there exists a peak below 10 eV. A possible explanation involves charge transfer collisions between Ar^+ and Ar. The resonant charge transfer cross section for $Ar^+ + Ar$ collisions is very large and increases with decreasing collision energy.[12] This type of charge transfer does not alter the ion identity but produces ions with significantly reduced energies.

The ion energy distributions in the period from rf turn off to the establishment of the quasistable E mode are more complicated. Figure 8 shows how the IEDs of CF_3^+ ions change with time from $t=0$ to $t=0.7$ ms. The IED obtained at $t=0$ shows a typical distribution during a 0.1 ms time window in the H mode. The small peak near 0 eV can be attributed in part to dissociative charge transfer collisions of CF_3^+ with CF_4 near the ion sampling pinhole yielding slow CF_3^+. The rf turn-off occurs during the period when the IED for $t=0.1$ ms was acquired. As can be seen in the figure, the high energy peak of the IED at $t=0.1$ ms centered at 16 eV decreases by about a factor of two compared to the IED at $t=0$. The low energy peak increases considerably, accompanied by the appearance of a long tail bridging the two peaks. Part of the high energy peak undoubtedly results from the fact that the period used for acquiring the IED at $t=0.1$ ms covers a portion of the H mode plasma. However, the high

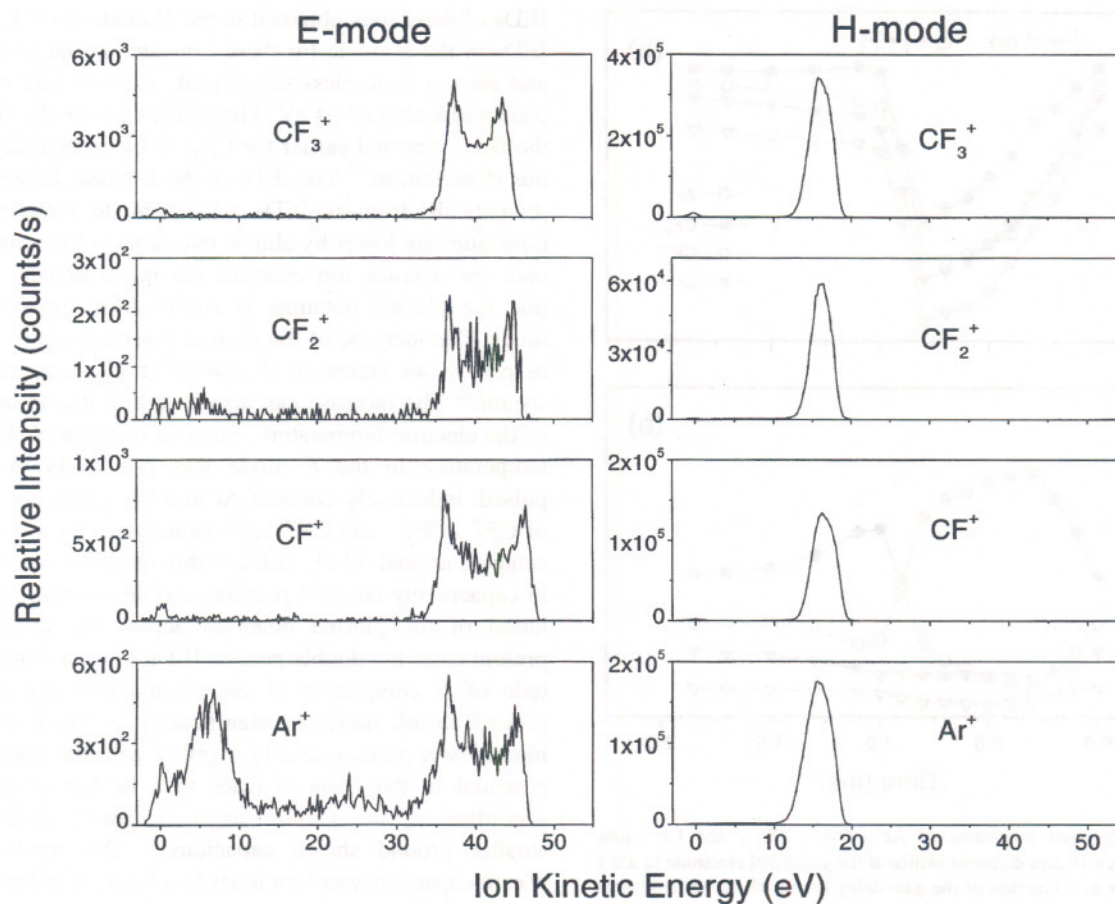FIG. 7. Typical IEDs for CF_3^+, CF_2^+, CF^+, and Ar^+ acquired in the E mode at $t = 0.7$ ms together with IEDs for these same ions obtained in the H mode at $t = 1.5$ ms.
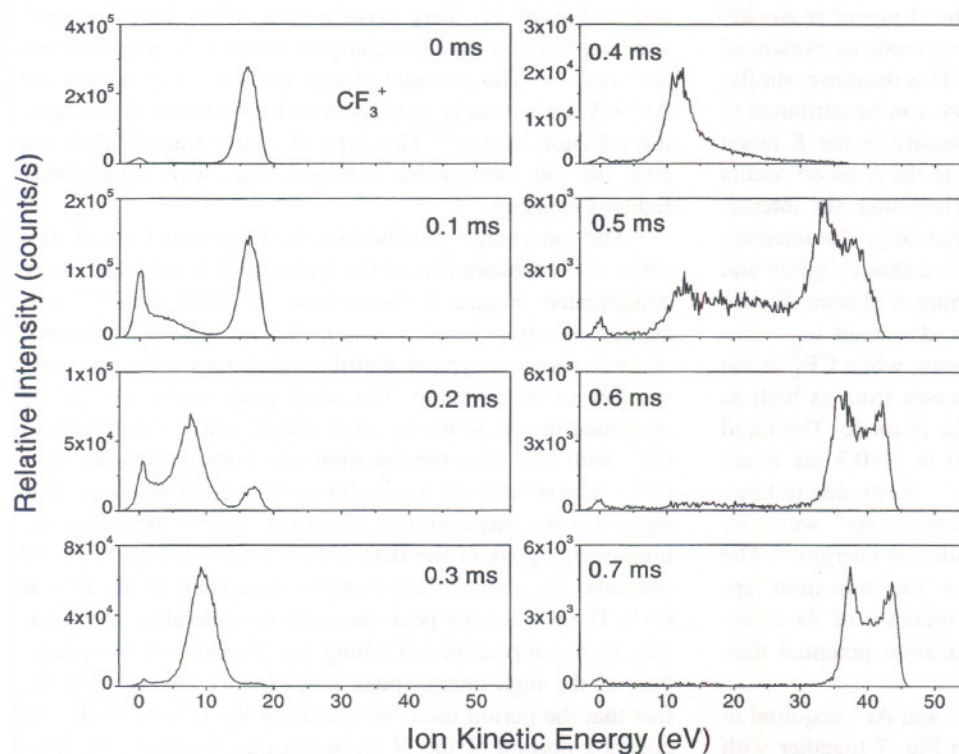

FIG. 8. Evolution of the IED for CF_3^+ ions from $t = 0$ to $t = 0.7$ ms.

energy peak can not entirely be attributed to the H mode because the same peak still exists at $t=0.2$ ms. Thus, if we were able to perfectly align the time window for measuring IED with the rf off period, the resultant IED would be similar to the IED shown for $t=0.1$ ms, except that the high energy peak would be significantly lower.

That the high energy peak continues to exist during the rf off period is an interesting feature which might seem to contradict the well-accepted notion that the electrons in the afterglow quickly cool off and therefore the plasma potential, if any, should be considerably lower than during the rf on period. Time-resolved Langmuir probe measurements in similar plasmas indeed show that the plasma potential decreases dramatically during the rf off period.[5] A cold plasma in the afterglow, however, has some fundamental differences from a normal rf-sustained plasma and could be significantly perturbed by a floating object such as a Langmuir probe. With continuous excitation, the potential drop between the plasma body and a floating object occurs mainly across the sheath outside the floating object and the potential variation within the plasma body is relatively small. The sheath voltage maintains net zero current to the floating object. In the afterglow, on the other hand, the dominant mechanism that maintains net zero current to a floating object is the ambipolar diffusion around the object, resulting in an electric field that restrains the electrons and anions and accelerates the positive ions to equalize their diffusion rates.[24] The potential drop within the cold plasma around the floating object resulting from this ambipolar field could be significantly more than the sheath potential drop, if any, outside the floating object.

The present results indicate that when the rf excitation is turned off, the sheath electric field is quickly replaced by the ambipolar electric field which extends deep into the plasma body. The high energy peak of the IED during the rf off period results from the ions originating from the center of the plasma without suffering charge transfer collisions on their path to the ground electrode. The low energy peak, on the other hand, is attributed to ions originating near the ground electrode and ions from the interior of the plasma that encounter a series of charge transfer collisions as they drift towards the electrode.

The rf excitation is turned on again during the period when the IED for $t=0.2$ ms is recorded. As can be seen in the figure, a new peak in the IED appears at about 7.5 eV. This new peak becomes dominant, with its peak position shifting towards higher energy, as the delay time increases from 0.2 to 0.4 ms, signifying an intermediate plasma state in which well-defined plasma sheaths are not yet established. The sheath structure for the E mode appears during the period when the IED for $t=0.5$ ms is recorded. Thereafter, the double-peaked IEDs, typical of capacitively-coupled discharges, can be clearly seen. It is interesting to note that the double peak shifts towards higher energy from $t=0.5$ to $t=0.7$ ms, indicating that the electron temperature continues to increase in the plasma.

IV. CONCLUSIONS

In agreement with the earlier observations in pulse-modulated inductively coupled plasmas in Cl_2 and Ar,[6] the present work shows that the pulsed plasmas in CF_4:Ar mixtures start in the E mode as each rf pulse is applied. The present work also reveals that the plasma transition from the E mode to the H mode can be delayed for as long as 0.75 ms under some plasma conditions. The delay may be partly due to an increased electron attachment rate during the afterglow, resulting in a space charge dominated by negative and positive ions. This kind of space charge can contribute to the delay in the mode transition because it increases the electron loss rate. The long delay in the mode transition allows us to perform not only time-resolved measurements of optical emission and electrical characteristics but also time-resolved measurements of ion energy distributions at the grounded electrode. These measurements show that a relatively short rf off period can severely perturb the plasma state and the recovery of the equilibrium plasma state, in general, takes much longer time than the rf off period. The time-resolved IEDs reveal rich plasma dynamics in the pulsed CF_4:Ar plasmas. The plasma potential in the E mode is significantly higher than in the H mode and increases as the $E \rightarrow H$ transition approaches. The ion intensities of Ar^+, CF_3^+, CF_2^+, and CF^+ continue to decrease after the turn on of the rf power due to the much lower equilibrium plasma density in the E mode than in the H mode. The fraction of Ar^+ ions increases dramatically before the transition occurs, indicating the importance of Ar metastables in the plasma mode transition. The time resolved IEDs also reveal the surprising result that the potential at the plasma center does not decrease in the afterglow in the time frame investigated.

An understanding of the "delayed" mode transition as observed in pulsed CF_4:Ar plasmas is important to better understand and ultimately control pulsed plasmas. Time-resolved ion energy, electrical and optical emission measurements provide complementary information on the plasma processes during pulsing. Optical and electrical measurements can provide high temporal resolution, nonperturbing diagnostics suitable for use as real- or in-time process control parameters. Ion energy measurements have a much lower time resolution, but provide important information concerning species identification and energy distributions of ion fluxes within the plasma.

[1] S. Samukawa, Jpn. J. Appl. Phys., Part 1 **33**, 2133 (1994).
[2] H. Sugai, T. H. Ahn, I. Ghanashev, M. Goto, M. Nagatsu, K. Nakamura, K. Suzuki, and H. Toyoda, Plasma Phys. Controlled Fusion **39**, A445 (1997).
[3] T. H. Ahn, K. Nakamura, and H. Sugai, Plasma Sources Sci. Technol. **5**, 139 (1996).
[4] C. Charles and R. W. Boswell, J. Appl. Phys. **78**, 766 (1995).
[5] S. Ashida, M. R. Shim, and M. A. Lieberman, J. Vac. Sci. Technol. A **14**, 391 (1996).
[6] G. A. Hebner and C. B. Fleddermann, J. Appl. Phys. **82**, 2814 (1997).
[7] P. J. Hargis et al., Rev. Sci. Instrum. **65**, 140 (1994).
[8] P. A. Miller, G. A. Hebner, K. E. Greenberg, P. D. Pochan, and B. P. Aragon, J. Res. Natl. Inst. Stand. Technol. **100**, 427 (1995).
[9] Y. Wang and J. K. Olthoff, J. Appl. Phys. **85**, 6358 (1999).
[10] J. R. Roberts, J. Res. Natl. Inst. Stand. Technol. **100**, 353 (1995).

[11] J. K. Olthoff and Y. Wang, J. Vac. Sci. Technol. A **17**, 1552 (1999).

[12] M. W. V. S. Rao, R. J. V. Brunt, and J. K. Olthoff, Phys. Rev. E **54**, 5641 (1996).

[13] B. E. Cherrington and L. J. Overzet, Bull. Am. Phys. Soc. **42**, 1712 (1997).

[14] E. C. Benck, A. Schwabedissen, A. Gates, and J. R. Roberts, J. Vac. Sci. Technol. A **16**, 306 (1998).

[15] M. V. Malyshev and M. V. Donnelly, J. Vac. Sci. Technol. A **15**, 550 (1997).

[16] R. Foest, J. K. Olthoff, R. J. V. Brunt, E. C. Benck, and J. R. Roberts, Phys. Rev. E **54**, 1876 (1996).

[17] R. E. H. Clark, private communication.

[18] I. M. El-Fayoumi, I. R. Jones, and M. M. Turner, J. Phys. D: Appl. Phys. **31**, 3082 (1998).

[19] U. Kortshagen, N. D. Gibson, and J. E. Lawler, J. Phys. D: Appl. Phys. **29**, 1224 (1996).

[20] K. Suzuki, K. Nakamura, H. Ohkubo, and H. Sugai, Plasma Sources Sci. Technol. **7**, 13 (1998).

[21] E. R. Fisher, M. E. Weber, and P. B. Armentrout, J. Chem. Phys. **92**, 2296 (1989).

[22] Y. Wang, Appl. Phys. Lett. **66**, 2186 (1995).

[23] B. Chapman, *Glow Discharge Processes* (Wiley, New York, 1980).

[24] M. A. Liberman and A. J. Lichtenberg, *Principles of Plasma Discharge and Materials Processing* (Wiley, New York, 1994).